공학 학사 학위논문

ISI Pre-equalization Techniques for Ultra-Wideband mmWave MIMO Communications (초고주파 초광대역 MIMO 통신을 위한 ISI pre-equalization 기법)

2025년 12월

서울대학교 공과대학

전기·정보공학부

김 주 호

ISI Pre-equalization Techniques for Ultra-Wideband mmWave MIMO Communications

(초고주파 초광대역 MIMO 통신을 위한 ISI pre-equalization 기법)

지도교수 최 완

이 논문을 공학 학사학위 논문으로 제출함.

서울대학교 공과대학

전기·정보공학부

김 주 호

김주호의 학사 학위 논문을 인준함.

2025년 12월 15일

지도교수 최 완 (인)

ABSTRACT

Delay Alignment Modulation (DAM) is a promising technique for mitigating Inter-Symbol Interference (ISI) in millimeter-wave (mmWave) and Terahertz (THz) communications by leveraging the channel's multi-path sparsity. While previous research has established the theoretical benefits of DAM, practical implementation faces two significant challenges: the hardware constraints of hybrid analog/digital beamforming and the physical reality of the spatial wideband effect, also known as beam squint. In large-scale antenna arrays with wide bandwidths, the spatial wideband effect introduces frequency-dependent phase shifts that manifest as distinct propagation delays for each antenna element, violating the standard narrowband assumption.

This thesis investigates the impact of channel model accuracy on the design of practical hybrid beamformers for DAM systems. We formulate and compare three distinct channel models: the conventional narrowband model (NB-DAM), which ignores per-antenna delays; the ground-truth wideband model (WB-DAM), which fully accounts for them; and a proposed sub-array approximation (SA-DAM). Using the Orthogonal Matching Pursuit (OMP) algorithm, we design hybrid beamformers based on each model and evaluate their performance in terms of achievable rate. Our simulation results demonstrate that the conventional narrowband model fails catastrophically as the number of antennas or system bandwidth increases, as it designs a beamformer that cannot cancel the true wideband ISI. Conversely, the proposed sub-array approximation (SA-DAM) is shown to be highly effective, achieving near-optimal performance comparable to the full wideband model while offering a computationally efficient solution for practical large-scale mmWave systems.

Keywords: Delay Alignment Modulation (DAM), Hybrid Beamforming, Spatial Wideband Effect, Inter-Symbol Interference (ISI), mmWave Communications, Sub-array Architecture

Contents

List of Tables

List of Figures

Chapter 1 Introduction

1.1 Background and Motivation

The exponential growth in global mobile data traffic is driving the evolution of wireless communication systems towards the sixth generation (6G). To meet the stringent requirements for ultra-high data rates and massive capacity, researchers are increasingly exploring the underutilized millimeter-wave (mmWave) and Terahertz (THz) frequency bands [1]. These bands offer vast amounts of available bandwidth, enabling multi-gigabit-per-second transmission speeds.

However, utilizing these high-frequency bands presents significant challenges. Signal propagation at mmWave and THz frequencies suffers from high path loss and severe atmospheric absorption. To compensate for this attenuation, transmitters must employ large-scale antenna arrays (Massive MIMO) to generate highly directional beams with high array gains. Consequently, future communication systems will be characterized by two defining features: **extremely wide bandwidths** and **extremely large antenna apertures**.

In wideband transmission, the symbol duration (T_s) becomes extremely short. When such signals propagate through a multi-path environment, the delay spread of the channel often exceeds the symbol duration, causing severe Inter-Symbol Interference (ISI). If left unmitigated, ISI destroys the orthogonality of the transmitted symbols, leading to an irreducible error floor.

Orthogonal Frequency Division Multiplexing (OFDM) is currently the dominant technique for handling ISI. By converting a frequency-selective wideband channel into multiple flat-fading narrowband subcarriers, OFDM effectively mitigates ISI. However, OFDM suffers from well-known drawbacks, including a high Peak-to-Average Power Ratio (PAPR) and sensitivity to carrier frequency offsets, which are particularly problematic for power-constrained mmWave/ THz systems [1].

Recently, **Delay Alignment Modulation (DAM)** has emerged as a promising alternative. By leveraging the spatial sparsity of mmWave channels and the high spatial resolution of large antenna arrays, DAM proactively aligns multi-path components at the receiver side, effectively

eliminating ISI without the drawbacks of OFDM.

1.2 Problem Statement

While the theoretical potential of DAM is well-established, its practical implementation faces a critical physical constraint that is often overlooked in existing literature: the **spatial wideband effect**, also known as "beam squint."

Most conventional research relies on the **narrowband assumption**, which assumes that the propagation delay of a signal is identical across all elements of an antenna array. While valid for small arrays or narrow bandwidths, this assumption breaks down in wideband massive MIMO systems. For a large array, the physical travel time of a wavefront across the array aperture can be significant relative to the short symbol period. This results in a frequency-dependent phase shift that causes the beam to "squint" or point in different directions for different frequencies.

This thesis addresses a fundamental gap in the design of practical **hybrid beamforming** systems for DAM. When a hybrid beamformer is designed using the conventional narrowband model (which ignores these per-antenna delays), it fails to align the channel taps correctly in a real-world wideband environment. This mismatch between the assumed model and physical reality can lead to severe performance degradation, rendering the system ineffective.

1.3 Thesis Contribution

The primary objective of this thesis is to investigate the impact of the spatial wideband effect on DAM performance and to validate a practical modeling approach that overcomes it. The main contributions are summarized as follows:

1. **Quantification of Narrowband Model Failure:** We rigorously analyze the performance of hybrid beamformers designed under the conventional narrowband assumption ('NB-DAM'). Through extensive simulations, we demonstrate that this model fails catastrophically as the number of antennas or system bandwidth increases, identifying the mechanism of failure as un-cancelled wideband ISI.

2. **Validation of Sub-Array Architecture:** We propose and evaluate a sub-array based channel approximation ('SA-DAM') as a practical solution. We demonstrate that by partitioning the large array into smaller sub-blocks, we can capture the essential spatial wideband characteristics with significantly reduced computational complexity compared to a full per-antenna model ('WB-DAM').

3. **Performance Analysis of Hybrid Beamforming:** Using the Orthogonal Matching Pursuit (OMP) algorithm, we verify that a practical hybrid architecture with a limited number of RF chains is sufficient to achieve near-optimal performance, provided the beamformer is designed using an accurate (wideband or sub-array) channel model.

1.4 Thesis Organization

The remainder of this thesis is organized as follows:

- **Chapter 2** reviews the fundamental principles of multi-path channels, the mechanism of Delay Alignment Modulation (DAM), and the mathematical formulation of the spatial wideband effect.
- **Chapter 3** defines the system architecture and explicitly formulates the three channel models (NB, SA, and WB) used in this study.
- **Chapter 4** details the proposed hybrid beamforming design methodology, including the derivation of the ideal MMSE beamformer and the OMP approximation algorithm.
- **Chapter 5** presents the simulation results, analyzing the achievable rate with respect to SNR, antenna number, and bandwidth, as well as a runtime complexity analysis.
- **Chapter 6** summarizes the findings and concludes the thesis.

Chapter 2 Background and Prior Research

2.1 The Multi-Path Channel Model and Inter-Symbol Interference (ISI)

In wireless communications, the transmitted signal rarely travels along a single, direct line-of-sight path. Instead, the signal reflects and scatters off surfaces such as buildings, walls, and other objects, creating multiple copies of the signal that arrive at the receiver at different times. This phenomenon is known as multi-path propagation.

To accurately represent this, we use a multi-path channel model. The channel is modeled as having L distinct paths. Each l-th path is characterized by its complex gain α_l, physical propagation delay τ_l, and an angle of departure (AoD) θ_{li}. Furthermore, each path l may itself consist of μ_l non-resolvable sub-paths. The total channel vector for the l-th path, $\mathbf{h}_l$, is therefore a composite of all its sub-paths [1].

$$\mathbf{h}_l = \alpha_l \sum_{i=1}^{\mu_l} v_{li} \mathbf{a}_t(\theta_{li}) \tag{2.1}$$

Here, v_{li} is the complex coefficient of the i-th sub-path within the l-th path, and $\mathbf{a}_t(\theta_{li})$ is the transmit array response vector corresponding to the AoD θ_{li}. For a Uniform Linear Array (ULA) with M_t antennas, the array response vector is defined in (2.2). d is the antenna spacing and λ is the wavelength. The array response vector captures the phase shifts across the antenna array due to the angle of departure, resulting in a channel vector $\mathbf{h}_l$ for that path.

$$\mathbf{a}_t(\theta_{li}) = \begin{bmatrix} 1 \\ e^{-j2\pi \frac{d}{\lambda} \sin(\theta_{li})} \\ \vdots \\ e^{-j2\pi(M_t-1) \frac{d}{\lambda} \sin(\theta_{li})} \end{bmatrix} \tag{2.2}$$

When a signal $\mathbf{x}[n]$ is transmitted using a pulse-shaping filter $p(t)$, the continuous-time channel is sampled at the receiver. This results in a discrete, tap-based channel model, $\mathbf{h}_{\mathrm{DL}}^H[q]$,

where q is the tap index. The tap-based channel model is highly general, as it naturally accounts for fractional path delays (where τ_l is not an integer multiple of the symbol duration T_s). As shown in (2.3)[1], the q-th tap of the channel is the superposition of contributions from all L paths.

$$\mathbf{h}_{\mathrm{DL}}^{H}[q] = \sum_{l=1}^{L} \mathbf{h}_{l}^{H} p(qT_s - \tau_l), q = 0, \cdots, Q \tag{2.3}$$

The total received signal $y[n]$ is the convolution of the transmitted signal $\mathbf{x}[n]$ with the channel taps $\mathbf{h}_{\mathrm{DL}}^{H}[q]$, plus additive noise $\mathbf{z}[n]$, as shown in (2.4)[1].

$$y[n] = \sum_{q=0}^{Q} \mathbf{h}_{\mathrm{DL}}^{H}[q]\mathbf{x}[n-q] + z[n] \tag{2.4}$$

2.2 Delay Alignment Modulation (DAM) with Hybrid Beamforming

The core principle of Delay Alignment Modulation (DAM) is to mitigate the ISI caused by multi-path propagation (as seen in (2.4)) by using two techniques at the transmitter: **delay pre-compensation** and **path-based beamforming** [1]. In a practical system with a hybrid architecture, the transmitted signal $\mathbf{x}[n]$ is formed as a superposition of L' delayed and beamformed symbols. L' is the number of dominant, resolvable paths (or clusters) that we choose to align. The signal is shown in (2.5).

$$\mathbf{x}[n] = \mathbf{F}_{\mathrm{RF}} \sum_{l=1}^{L'} \mathbf{f}_{\mathrm{BB},l} s[n - \kappa_l] \tag{2.5}$$

Here, $\mathbf{F}_{\mathrm{RF}}$ is the $M_t \times M_{\mathrm{RF}}$ analog beamforming matrix, $\mathbf{f}_{\mathrm{BB},l}$ is the $M_{\mathrm{RF}} \times 1$ digital beamforming vector for the l-th path, $s[n]$ is the data symbol, and κ_l is the intentional pre-delay applied to the l-th path. Substituting this signal into our tap-based channel model (2.4) gives the received signal in (2.6).

$$y[n] = \sum_{q=0}^{Q} \sum_{l=1}^{L'} \mathbf{h}_{\mathrm{DL}}^{H}[q]\mathbf{F}_{\mathrm{RF}}\mathbf{f}_{\mathrm{BB},l} s[n - \kappa_l - q] + z[n] \tag{2.6}$$

Solving for $\mathbf{F}_{\mathrm{RF}}$ and $\mathbf{f}_{\mathrm{BB},l}$ jointly is complex. To find the optimal beamformer, we first consider the ideal, unconstrained fully-digital beamformer $\mathbf{f}_l \in \mathbb{C}^{M_t \times 1}$, where $\mathbf{f}_l = \mathbf{F}_{\mathrm{RF}}\mathbf{f}_{\mathrm{BB},l}$. This $\mathbf{f}_l$ will serve as the optimal target for our hybrid approximation in the next chapter.

The key to DAM is to select the pre-delays κ_l to align the L' strongest taps $\{q_l\}_{l=1}^{L'}$ at a single time instant. We set $\kappa_l = q_{\max} - q_l$, where $q_{\max} = \max(q_l)$. This forces all desired signal components to arrive at the receiver at time $n - q_{\max}$.

With this substitution, the received signal can be decomposed into its desired part and the residual ISI, as shown in (2.7).

$$y[n] = \left\{ \sum_{l=1}^{L'} \mathbf{h}_{\mathrm{DL}}^H[q_l]\mathbf{f}_l \right\} s[n - q_{max}] + \sum_{l=1}^{L'} \sum_{q \neq q_l}^{Q} \mathbf{h}_{\mathrm{DL}}^H[q]\mathbf{f}_l s[n - q_{max} + q_l - q] + z[n] \tag{2.7}$$

To analyze the ISI term, we group all signal components that arrive at the same time offset $i = q_l - q$. We define the effective ISI channel $\mathbf{g}_l^H[i]$ as the contribution of the l-th path beamformer to the i-th ISI tap, as shown in (2.8).

$$\mathbf{g}_l^H[i] = \begin{cases} \mathbf{h}_{\mathrm{DL}}^H[q], & \text{if } \exists\, l \in \{1, \ldots, L'\} \text{ s.t. } q_l - q = i, \\ \mathbf{0}, & \text{otherwise.} \end{cases} \tag{2.8}$$

Using this definition, the received signal can be rewritten in the clean form of (2.9), which explicitly separates the desired signal at $n - q_{\max}$ from the ISI at all other time offsets $i \neq 0$.

$$y[n] = \left(\sum_{l=1}^{L'} \mathbf{h}_{\mathrm{DL}}^H[q_l]\mathbf{f}_l \right) s[n - q_{\max}] + \sum_{\substack{i=-Q \\ i \neq 0}}^{Q} \left(\sum_{l=1}^{L'} \mathbf{g}_l^H[i]\mathbf{f}_l \right) s[n - q_{\max} + i] + z[n]. \tag{2.9}$$

From this, the Signal-to-Interference-plus-Noise Ratio (SINR) is the power of the desired signal divided by the sum of the power of all ISI taps and the noise power σ^2.

$$\gamma = \frac{\left| \sum_{l=1}^{L'} \mathbf{h}_{\mathrm{DL}}^H[q_l]\mathbf{f}_l \right|^2}{\sum\limits_{\substack{i=-Q \\ i \neq 0}}^{Q} \left| \sum\limits_{l=1}^{L'} \mathbf{g}_l^H[i]\mathbf{f}_l \right|^2 + \sigma^2} = \frac{\bar{\mathbf{f}}^H \bar{\mathbf{h}}_{\mathrm{DL}} \bar{\mathbf{h}}_{\mathrm{DL}}^H \bar{\mathbf{f}}}{\bar{\mathbf{f}}^H \left(\sum\limits_{\substack{i=-Q \\ i \neq 0}}^{Q} \bar{\mathbf{g}}[i]\bar{\mathbf{g}}^H[i] + \sigma^2 \mathbf{I}/\|\bar{\mathbf{f}}\|^2 \right) \bar{\mathbf{f}}}. \tag{2.10}$$

To solve for the optimal beamformer $\bar{\mathbf{f}}$, the SINR is written in a vectorized form using the stacked vectors $\bar{\mathbf{h}}_{\mathrm{DL}}$, $\bar{\mathbf{f}}$, and $\bar{\mathbf{g}}[i]$, where $\bar{\mathbf{h}}_{\mathrm{DL}} = [\mathbf{h}_{\mathrm{DL}}^T[q_1], \ldots, \mathbf{h}_{\mathrm{DL}}^T[q_{L'}]]^T \in \mathbb{C}^{M_t L' \times 1}$, $\bar{\mathbf{f}} = [\mathbf{f}_1^T, \ldots, \mathbf{f}_{L'}^T]^T \in \mathbb{C}^{M_t L' \times 1}$, and $\mathbf{g}[i] = [\mathbf{g}_1^T[i], \ldots, \mathbf{g}_{L'}^T[i]]^T \in \mathbb{C}^{M_t L' \times 1}$. To maximize the spectral efficiency, we must maximize this SINR. The vector $\bar{\mathbf{f}}$ that maximizes this expression is the well-known Minimum Mean Square Error (MMSE) solution [1], given by (2.11).

$$\bar{\mathbf{f}}^{\mathrm{MMSE}} = \sqrt{P} \frac{\mathbf{C}^{-1} \bar{\mathbf{h}}_{\mathrm{DL}}}{\left\| \mathbf{C}^{-1} \bar{\mathbf{h}}_{\mathrm{DL}} \right\|} \tag{2.11}$$

where $\mathbf{C} \triangleq \sum_{i=-Q, i \neq 0}^{Q} \bar{\mathbf{g}}[i] \bar{\mathbf{g}}^H[i] + \sigma^2 / P \mathbf{I}$, assuming the total transmit power is $\|\bar{\mathbf{f}}\|^2 = P$. This $\bar{\mathbf{f}}^{\mathrm{MMSE}}$ represents the optimal, fully-digital beamformer that serves as the target for our practical hybrid design.

2.3 The Spatial Wideband Effect

The channel model presented so far, the tap-based model in (2.3), is based on a critical simplifying assumption: the **narrowband assumption**. This assumption presumes that the signal's symbol period T_s is much larger than the propagation delay of the signal across the entire antenna array. In this case, a signal from a given path l is treated as arriving at all M_t antennas at the exact same time instant, τ_l.

However, in mmWave and THz systems, this assumption breaks down. The combination of very wide bandwidths (which leads to a very short symbol period T_s) and very large antenna arrays (large M_t, which means a large physical aperture) creates a new challenge known as the **spatial wideband effect**, or "beam squint."

This effect is a simple consequence of geometry. For a Uniform Linear Array (ULA), a planar wavefront arriving from an angle of departure θ_{li} does not hit all antennas simultaneously. It hits one end of the array (e.g., antenna $m = 1$) first, and then must travel an additional distance to reach the other antennas.

The additional distance the signal must travel to reach antenna m (relative to antenna 1) is

$(m-1)d\sin(\theta_{li})$. This creates a small, per-antenna time delay, $\Delta\tau_m$, as shown in (2.12) [2].

$$\Delta\tau_m = (m-1)\frac{d\sin(\theta_{li})}{c} \tag{2.12}$$

Therefore, the true physical delay for the m-th antenna of the l-th path, $\tau_{l,m}$, is not constant with respect to the antenna index. The total delay is given by (2.13).

$$\tau_{l,m} = \tau_{l,1} + \Delta\tau_m = \tau_{l,1} + (m-1)\frac{d\sin(\theta_{li})}{c} \tag{2.13}$$

This per-antenna delay $\tau_{l,m}$ has a severe impact on the system, which is the central problem this thesis investigates:

1. **In the Frequency Domain (Beam Squint):** A time delay $\Delta\tau_m$ is equivalent to a frequency-dependent phase shift $e^{-j2\pi f\Delta\tau_m}$. In a wideband system, the frequency f varies across the band (e.g., $f \in [f_c - B/2, f_c + B/2]$). This means the phase shift applied to the low-frequency components of the signal is different from the phase shift applied to the high-frequency components. As a result, the beamformer physically "points" in a slightly different direction for different frequencies, an effect known as beam squint.

2. **In the Time Domain (Tap-Based Channel Smearing):** More critically for DAM, this effect changes the fundamental structure of the tap-based channel model. The model in (2.3) is incorrect because it assumes the entire vector $\mathbf{h}_l$ is multiplied by a single pulse $p(qT_s - \tau_l)$. The true wideband channel model, which we will define in Chapter 3, must account for the fact that each element m of the antenna array has its own distinct delay $\tau_{l,m}$.

This "smearing" of a single path's energy across both time (taps) and space (antennas) is the true wideband channel. Failing to model it correctly—as the conventional 'NB-DAM' model does—will result in a flawed beamformer design that fails to align the channel taps, leading to massive residual ISI. This thesis will quantify this performance loss and demonstrate how to correct it using more accurate channel models.

Chapter 3 System and Channel Model

3.1 System Architecture

We consider a single-user downlink communication system, as is standard in foundational DAM research [1]. The system consists of:

- A **Base Station (BS)** (transmitter) equipped with a large-scale Uniform Linear Array (ULA) of M_t antenna elements.
- A **User Equipment (UE)** (receiver) equipped with a single antenna.

This configuration is known as a Multiple-Input Single-Output (MISO) system.

The key challenge in practical mmWave and THz systems is the cost and power consumption of the Radio Frequency (RF) components. An ideal, fully-digital (FD) beamformer would require a dedicated RF chain for each of the M_t antennas. This is prohibitively expensive for large M_t.

To address this, we adopt a practical **Hybrid Analog/Digital architecture**.

In this architecture, the BS is equipped with only M_{RF} RF chains, where $M_{\text{RF}} \ll M_t$. The beamforming task is split into two stages:

1. **Analog Beamformer ($\mathbf{F_{RF}}$):** A high-dimensional ($M_t \times M_{\text{RF}}$) matrix implemented by analog phase shifters. This stage performs spatial pre-coding in the analog domain. Its key hardware constraint is that all its elements must have a constant modulus (i.e., they can only change phase, not amplitude).
2. **Digital Beamformer ($\mathbf{F_{BB}}$):** A low-dimensional ($M_{\text{RF}} \times L'$) matrix implemented in the digital baseband, where L' is the number of taps to be aligned. This stage performs more complex beamforming.

The overall effective beamforming vector for the l-th tap, $\mathbf{f}_l$, is the product of these two stages: $\mathbf{f}_l = \mathbf{F}_{\text{RF}}\mathbf{f}_{\text{BB},l}$. This structure leads directly to the transmitted signal model we use throughout this thesis, as previously shown in (2.5).

3.2 Channel Model Formulations

We introduce three channel models: NB-DAM, WB-DAM, and SA-DAM. NB-DAM is the conventional narrowband model, ignoring the spatial wideband effect. It assumes that a signal arrives at all M_t antennas at the exact same physical delay τ_l. This model corresponds to the standard formulation in (2.3). NB-DAM is physically inaccurate for large antenna arrays and wide bandwidths, as the travel time is different for each antenna.

WB-DAM is the "physically perfect" ground truth model, fully capturing the spatial wideband effect. It correctly calculates the unique, distinct delay for every single antenna in the array. The delay for the m-th antenna of the l-th path is given by (3.1)[2],

$$\tau_{l,m} = \tau_{l,1} + (m-1)\frac{d\sin(\theta_{li})}{c}, m = 1, \cdots, M_t \tag{3.1}$$

where c is the speed of light. The q-th tap of the WB-DAM channel is given by (3.2).

$$\mathbf{h}^H_{\text{WB-DAM}}[q] = \sum_{l=1}^{L}\sum_{i=1}^{\mu_l} \overline{\alpha_l v_{li}} \left[p(qT_s - \tau_{l,1}), \quad \cdots, \quad e^{j\frac{2\pi(M_t-1)d}{\lambda}\sin(\theta_{li})} p(qT_s - \tau_{l,M_t}) \right] \tag{3.2}$$

The SA-DAM model is an approximation of the WB-DAM model, quantizing the spatial delay across the array. The M_t antenna array is partitioned into K sub-arrays, each with $M_s = M_t/K$ antennas. Each sub-array assumes a common delay for all its antennas, specifically the delay of the first antenna in that sub-array. The delay for the k-th sub-array of the l-th path is given by (3.3), and the q-th tap of the SA-DAM channel is given by (3.4).

$$\tau^{\text{rep}}_{l,k} = \tau_{l,1} + (k-1)M_s\frac{d\sin(\theta_{li})}{c}, k = 1, \cdots, K \tag{3.3}$$

$$\mathbf{h}_{\mathrm{SA-DAM}}^{H}[q] = \sum_{l=1}^{L}\sum_{i=1}^{\mu_l}\overline{\alpha_l v_{li}} \cdot \Bigg[\underbrace{p(qT_s - \tau_{l,1}^{\mathrm{rep}}), \ldots, e^{j2\pi(M_s-1)\frac{d}{\lambda}\sin(\theta_{li})}p(qT_s - \tau_{l,1}^{\mathrm{rep}})}_{\text{Sub-array 1 (uses delay } \tau_{l,1}^{\mathrm{rep}})}, \ldots,$$

$$\underbrace{e^{j2\pi(M_t-M_s)\frac{d}{\lambda}\sin(\theta_{li})}p(qT_s - \tau_{l,K}^{\mathrm{rep}}), \ldots, e^{j2\pi(M_t-1)\frac{d}{\lambda}\sin(\theta_{li})}p(qT_s - \tau_{l,K}^{\mathrm{rep}})}_{\text{Sub-array } K \text{ (uses delay } \tau_{l,K}^{\mathrm{rep}})}\Bigg] \tag{3.4}$$

3.3 Problem Formulation

The background research in Section 2.2 presents the optimal fully-digital beamformer, $\overline{\mathbf{f}}^{\mathrm{MMSE}}$ (from (2.11)), which maximizes the SINR in a tap-based DAM system. This solution, however, is purely theoretical as it assumes a dedicated Radio Frequency (RF) chain for each of the M_t antenna elements. In practical mmWave and THz systems, this fully-digital architecture is prohibitively expensive and power-intensive.

To address this, we employ a practical hybrid analog/digital architecture, as previously defined in (2.5). In this structure, the $M_t \times 1$ ideal beamformer $\mathbf{f}_l$ for each tap l is approximated by the product of a high-dimensional analog beamforming matrix $\mathbf{F}_{\mathrm{RF}} \in \mathbb{C}^{M_t \times M_{\mathrm{RF}}}$ and a low-dimensional digital beamforming vector $\mathbf{f}_{\mathrm{BB},l} \in \mathbb{C}^{M_{\mathrm{RF}} \times 1}$, where the number of RF chains $M_{\mathrm{RF}} \ll M_t$. Let $\mathbf{F}_{\mathrm{opt}} = [\mathbf{f}_1, \ldots, \mathbf{f}_{L'}] \in \mathbb{C}^{M_t \times L'}$ be the ideal, fully-digital beamforming matrix (composed of the MMSE vectors). The first challenge is to find the hybrid matrices $(\mathbf{F}_{\mathrm{RF}}, \mathbf{F}_{\mathrm{BB}})$ that best approximate $\mathbf{F}_{\mathrm{opt}}$. This is a matrix factorization problem:

$$\min_{\mathbf{F}_{\mathrm{RF}}, \mathbf{F}_{\mathrm{BB}}} \|\mathbf{F}_{\mathrm{opt}} - \mathbf{F}_{\mathrm{RF}}\mathbf{F}_{\mathrm{BB}}\|_F^2 \tag{3.5}$$

This optimization is subject to two critical hardware constraints:

1. The analog beamformer $\mathbf{F}_{\mathrm{RF}}$ must satisfy the **constant-modulus constraint**, as it is implemented by analog phase shifters which can only alter the phase, not the amplitude, of the signal [1].

2. The total transmitted power is constrained, i.e., $\|\mathbf{F}_{\mathrm{RF}}\mathbf{F}_{\mathrm{BB}}\|_F^2 = P$.

Here lies the central problem of this thesis. The "optimal" beamformer $\mathbf{F}_{\text{opt}}$ is not absolute; it is a function of the channel model $\mathbf{h}_{\text{DL}}[q]$ used to calculate it. As established in Section 3.2, we have three distinct channel models, each with a different level of physical accuracy:

- $\mathbf{h}_{\text{NB-DAM}}[q]$ (The inaccurate, narrowband model)
- $\mathbf{h}_{\text{SA-DAM}}[q]$ (The approximate, sub-array model)
- $\mathbf{h}_{\text{WB-DAM}}[q]$ (The "ground truth," wideband model)

This implies we can compute three different "ideal" beamformers:

$$\mathbf{F}_{\text{opt}}^{\text{NB}} = \text{MMSE}(\mathbf{h}_{\text{NB-DAM}}) \tag{3.6}$$

$$\mathbf{F}_{\text{opt}}^{\text{SA}} = \text{MMSE}(\mathbf{h}_{\text{SA-DAM}}) \tag{3.7}$$

$$\mathbf{F}_{\text{opt}}^{\text{WB}} = \text{MMSE}(\mathbf{h}_{\text{WB-DAM}}) \tag{3.8}$$

This leads to our primary research objective: **to quantify the performance mismatch when a practical hybrid beamformer is designed using an imperfect channel model.**

Our methodology, which will be detailed in Chapter 4 and 5, is as follows:

1. **Design:** For each of the three channel models, we first compute the ideal beamformer ($\mathbf{F}_{\text{opt}}^{\text{NB}}, \mathbf{F}_{\text{opt}}^{\text{SA}}, \mathbf{F}_{\text{opt}}^{\text{WB}}$). We then solve the approximation problem (3.5) to find a corresponding set of practical hybrid beamformers: $(\mathbf{F}_{\text{RF}}^{\text{NB}}, \mathbf{F}_{\text{BB}}^{\text{NB}})$, $(\mathbf{F}_{\text{RF}}^{\text{SA}}, \mathbf{F}_{\text{BB}}^{\text{SA}})$, and $(\mathbf{F}_{\text{RF}}^{\text{WB}}, \mathbf{F}_{\text{BB}}^{\text{WB}})$.

2. **Evaluation:** The ultimate goal is to maximize performance in the real world. Therefore, we evaluate all three hybrid beamformers on the single "ground truth" channel, $\mathbf{h}_{\text{WB-DAM}}$. For any given hybrid beamformer $(\mathbf{F}_{\text{RF}}, \mathbf{F}_{\text{BB}})$, the evaluated SINR is:

$$\gamma_{\text{eval}} = \frac{\left|\sum_{l=1}^{L'} \mathbf{h}_{\text{WB-DAM}}^{H}[q_l]\mathbf{F}_{\text{RF}}\mathbf{f}_{\text{BB},l}\right|^2}{\sum_{\substack{i=-Q \\ i\neq 0}}^{Q} \left|\sum_{l=1}^{L'} \mathbf{g}_{\text{WB-DAM},l}^{H}[i]\mathbf{F}_{\text{RF}}\mathbf{f}_{\text{BB},l}\right|^2 + \sigma^2} \tag{3.9}$$

   where $\mathbf{h}_{\text{WB-DAM}}^{H}[q]$ and $\mathbf{g}_{\text{WB-DAM},l}^{H}[i]$ are both derived from the true wideband channel model (3.2).

The final performance metric is the achievable rate $R = \log_2(1 + \gamma_{\text{eval}})$. This formulation allows us to directly quantify the performance loss from using the simpler, but physically inaccurate, 'NB-DAM' and 'SA-DAM' models for hybrid beamformer design.

Chapter 4 Proposed Hybrid Beamforming Design

As formulated in Section 3.3, our core task is to design a practical hybrid beamformer $(\mathbf{F}_{\mathrm{RF}}, \mathbf{F}_{\mathrm{BB}})$ that approximates an ideal, fully-digital target $\mathbf{F}_{\mathrm{opt}}$. This chapter details the specific two-stage methodology and algorithms used to achieve this.

First, we define the ideal target $\mathbf{F}_{\mathrm{opt}}$ by solving the fully-digital MMSE problem. Second, we describe the Orthogonal Matching Pursuit (OMP) algorithm, which is the sparse approximation technique used to solve the matrix factorization problem in (3.5). Finally, we detail the construction of the channel-aware beamforming dictionary, which is a critical component for the OMP algorithm's success.

4.1 Stage 1: Ideal Fully-Digital MMSE Beamformer

The first stage is to compute the theoretical "target" beamformer, $\mathbf{F}_{\mathrm{opt}}$, which we aim to approximate. This target is the optimal fully-digital beamformer that maximizes the SINR. As derived in Section 2.2, the SINR is maximized by the MMSE solution given in (2.11):

$$\bar{\mathbf{f}}^{\mathrm{MMSE}} = \sqrt{P}\frac{\mathbf{C}^{-1}\bar{\mathbf{h}}_{\mathrm{DL}}}{\left\|\mathbf{C}^{-1}\bar{\mathbf{h}}_{\mathrm{DL}}\right\|}$$

The resulting $\bar{\mathbf{f}}^{\mathrm{MMSE}}$ is a stacked vector of size $(M_t L' \times 1)$. To create our target matrix $\mathbf{F}_{\mathrm{opt}}$, we simply reshape this vector into an $(M_t \times L')$ matrix, where each l-th column corresponds to the ideal beamforming vector for the l-th selected tap. To address the problem defined in Section 3.3, this entire calculation is performed independently for each of the three channel models. This yields three distinct ideal beamforming matrices, which form the targets for our hybrid approximation:

- $\mathbf{F}_{\mathrm{opt}}^{\mathrm{NB}} = \mathrm{Reshape}(\mathrm{MMSE}(\mathbf{h}_{\text{NB-DAM}}))$
- $\mathbf{F}_{\mathrm{opt}}^{\mathrm{SA}} = \mathrm{Reshape}(\mathrm{MMSE}(\mathbf{h}_{\text{SA-DAM}}))$

- $\mathbf{F}_{\text{opt}}^{\text{WB}} = \text{Reshape}(\text{MMSE}(\mathbf{h}_{\text{WB-DAM}}))$

4.2 Stage 2: Hybrid Approximation via Orthogonal Matching Pursuit

With the ideal target $\mathbf{F}_{\text{opt}}$ defined, the second stage is to solve the practical approximation problem from (3.5). This involves finding the analog beamforming matrix $\mathbf{F}_{\text{RF}}$ and digital beamforming matrix $\mathbf{F}_{\text{BB}}$ that minimize the approximation error, subject to the hardware constraints.

This problem is non-convex due to the constant-modulus constraint on $\mathbf{F}_{\text{RF}}$. We solve it using a greedy sparse recovery algorithm, Orthogonal Matching Pursuit (OMP), which is well-suited for this task [3]. The OMP algorithm iteratively constructs the analog beamformer $\mathbf{F}_{\text{RF}}$ column by column.

The process is as follows:

1. **Initialization:** Start with an empty analog beamformer $\mathbf{F}_{\text{RF}}^{(0)}$ (a matrix with 0 columns) and set the residual matrix $\mathbf{F}_{\text{res}} = \mathbf{F}_{\text{opt}}$. Set the iteration counter $k = 1$.

2. **Atom Selection:** In the k-th iteration, find the "best" analog beam vector (or "atom") $\mathbf{a}_k$ from a predefined beamforming dictionary $\mathcal{A}_t$ (see Section 4.3). The best atom is the one that is most correlated with the current residual, i.e., it maximizes $\left\|\mathbf{a}^H \mathbf{F}_{\text{res}}\right\|_F^2$.

$$\mathbf{a}_k = \arg\max_{\mathbf{a} \in \mathcal{A}_t} \left\|\mathbf{a}^H \mathbf{F}_{\text{res}}\right\|_F^2 \tag{4.1}$$

3. **Update Analog Beamformer:** Add the selected atom to the analog beamformer: $\mathbf{F}_{\text{RF}}^{(k)} = [\mathbf{F}_{\text{RF}}^{(k-1)}, \mathbf{a}_k]$.

4. **Update Digital Beamformer:** Re-calculate the optimal digital beamformer $\mathbf{F}_{\text{BB}}^{(k)}$ by finding the regularized least-squares solution that projects $\mathbf{F}_{\text{opt}}$ onto the subspace now spanned by $\mathbf{F}_{\text{RF}}^{(k)}$:

$$\mathbf{F}_{\text{BB}}^{(k)} = \left((\mathbf{F}_{\text{RF}}^{(k)})^H \mathbf{F}_{\text{RF}}^{(k)} + \delta \mathbf{I}\right)^{-1} (\mathbf{F}_{\text{RF}}^{(k)})^H \mathbf{F}_{\text{opt}} \tag{4.2}$$

where δ is a small regularization factor for numerical stability.

5. **Update Residual:** Update the residual matrix to represent the remaining portion of $\mathbf{F}_{\text{opt}}$:

$$\mathbf{F}_{\text{res}} = \mathbf{F}_{\text{opt}} - \mathbf{F}_{\text{RF}}^{(k)}\mathbf{F}_{\text{BB}}^{(k)} \tag{4.3}$$

6. **Iteration:** Increment k and repeat from Step 2 until $k = M_{\text{RF}}$ (i.e., we have selected one analog beam for each RF chain).

7. **Finalization:** The final hybrid matrices are $\mathbf{F}_{\text{RF}} = \mathbf{F}_{\text{RF}}^{(M_{\text{RF}})}$ and $\mathbf{F}_{\text{BB}} = \mathbf{F}_{\text{BB}}^{(M_{\text{RF}})}$. The digital beamformer $\mathbf{F}_{\text{BB}}$ is then scaled to ensure the total power constraint $\|\mathbf{F}_{\text{RF}}\mathbf{F}_{\text{BB}}\|_F^2 = P$ is met.

4.3 Beamforming Dictionary Construction

The performance of the OMP algorithm is critically dependent on the quality of the beamforming dictionary $\mathcal{A}_t$. This dictionary is a finite set of $M_t \times 1$ vectors, representing all possible analog beams that the hardware can form.

A simple approach would be to populate $\mathcal{A}_t$ with array response vectors pointing in many different, finely-quantized directions. However, this creates a very large dictionary, making the search in Step 2 of the OMP algorithm computationally expensive.

Given that mmWave and THz channels are spatially sparse, with power concentrated along the L propagation paths, we adopt a more intelligent, channel-aware dictionary. We construct the dictionary $\mathcal{A}_t$ using the actual Angles of Departure (AoDs) of the channel's sub-paths.

The dictionary is formed by taking the set of all sub-path AoDs, $\{\theta_{li}\}$, from the physical channel model and creating an array response vector for each one:

$$\mathcal{A}_t = \{\mathbf{a}_t(\theta_{li}) \mid l \in [1, L], i \in [1, \mu_l]\} \tag{4.4}$$

This approach creates a compact and highly-relevant dictionary, ensuring that the OMP algorithm selects analog beams that are already pointed in directions where significant channel energy exists. In our simulation, if the number of paths is very small, we augment this dictionary with a standard quantized grid of angles to ensure full spatial coverage.

4.4 Complete Design and Evaluation Workflow

Our simulation script combines these stages into a complete workflow to test our central hypothesis. This workflow is executed for every single Monte Carlo realization to average out the effects of random channel generation.

The process is as follows:

1. **Generate Physical Channel:** A single set of physical parameters (path gains α_l, physical delays τ_l, and AoDs θ_{li}) is randomly generated.

2. **Instantiate All Models:** Using these physical parameters, all three channel models are computed and instantiated:

   - $\mathbf{h}_{\text{NB-DAM}}[q]$ (from (2.3))
   - $\mathbf{h}_{\text{SA-DAM}}[q]$ (from (3.4))
   - $\mathbf{h}_{\text{WB-DAM}}[q]$ (from (3.2))

3. **Create Dictionary:** A single channel-aware dictionary $\mathcal{A}_t$ is created from the physical AoDs $\{\theta_{li}\}$.

4. **Design Beamformers (in parallel):**

   (a) **(NB Design)** $\mathbf{F}_{\text{opt}}^{\text{NB}}$ is computed from $\mathbf{h}_{\text{NB-DAM}}$.
   OMP is then used to find $(\mathbf{F}_{\text{RF}}^{\text{NB}}, \mathbf{F}_{\text{BB}}^{\text{NB}})$.

   (b) **(SA Design)** $\mathbf{F}_{\text{opt}}^{\text{SA}}$ is computed from $\mathbf{h}_{\text{SA-DAM}}$.
   OMP is then used to find $(\mathbf{F}_{\text{RF}}^{\text{SA}}, \mathbf{F}_{\text{BB}}^{\text{SA}})$.

   (c) **(WB Design)** $\mathbf{F}_{\text{opt}}^{\text{WB}}$ is computed from $\mathbf{h}_{\text{WB-DAM}}$.
   OMP is then used to find $(\mathbf{F}_{\text{RF}}^{\text{WB}}, \mathbf{F}_{\text{BB}}^{\text{WB}})$.

5. **Evaluate on Ground Truth:** All three resulting hybrid beamformers are evaluated on the one, true channel model, $\mathbf{h}_{\text{WB-DAM}}$, by calculating their resulting SINR γ_{eval} using (3.9).

6. **Calculate Rate:** The final achievable rate $R = \log_2(1 + \gamma_{\text{eval}})$ is stored for all three designs.

This workflow ensures a fair and direct comparison. It isolates the performance difference caused purely by the choice of channel model used during the design stage. The results of this workflow are presented in the following chapter.

Chapter 5 Simulation Results and Analysis

In this chapter, we present the numerical results of our Monte Carlo simulations to evaluate the performance of the three DAM channel models: narrowband ('NB-DAM'), sub-array ('SA-DAM'), and the ground-truth wideband ('WB-DAM'). All simulations were conducted in MATLAB, and the results are averaged over 1000 independent channel realizations.

We conduct three main experiments to analyze the achievable rate (calculated as $R = \log_2(1+\gamma_{\text{eval}})$) under different system conditions:

1. **Achievable Rate vs. SNR**
2. **Achievable Rate vs. Number of Antennas (M_t)**
3. **Achievable Rate vs. System Bandwidth (B)**

In each experiment, one parameter is varied while all others are held at their default values, which are defined in the following section.

5.1 Simulation Environment and Parameters

The baseline simulation parameters are summarized in Table 5.1. These values are held constant unless specified otherwise in a particular experiment. The parameters are based on a typical mmWave communication scenario, consistent with the reference literature [1].

Our simulation's default setup assumes a 28 GHz mmWave system with a 128 MHz bandwidth. The transmitter is a large-scale ULA with $M_t = 128$ antennas and a practical hybrid architecture with $M_{\text{RF}} = 8$ RF chains. This corresponds to an $M_{\text{RF}}/L = 2$ ratio, which is noted in [1] as a region where hybrid beamforming can closely approximate fully-digital performance.

The channel is modeled with $L = 4$ sparse multi-paths, each with a single sub-path, distributed over a maximum delay spread of 1000 ns. The signal pulse shaping uses a standard Root-Raised Cosine (RRC) filter with a rolloff factor of $\beta = 0.22$. The default transmit power is normalized to $P = 1$, and the noise power is set to $\sigma^2 = 0.01$, resulting in a default SNR of 20 dB.

Table 5.1: Default Simulation Parameters

Parameter	**Symbol**	**Value**
System Parameters		
Number of Antennas (Default)	M_t	128
Number of RF Chains	M_{RF}	8
Carrier Frequency	f_c	28 GHz
System Bandwidth (Default)	B	128 MHz
Sampling Period (Default)	T_s	$1/B \approx 7.81$ ns
Antenna Spacing	d	$\lambda/2$
Normalized Transmit Power	P	1.0
Noise Power (Default)	σ^2	0.01
Default SNR (P/σ^2)	—	20 dB
Channel Model Parameters		
Number of Paths	L	4
Max Sub-Paths per Path	$\mu_{\max}$	1
Maximum Delay Spread	$\tau_{\max}$	1000 ns
Path AoD Distribution	θ_{li}	$U(-\pi/3, \pi/3)$
RRC Rolloff Factor	β	0.22
RRC Samples per Symbol	—	8
RRC Filter Taps	—	61
DAM & Simulation Parameters		
Tap Selection Threshold	C	0.01
Number of SA-DAM Sub-blocks	K	8
Monte Carlo Realizations	—	1000

Based on the default parameters in Table 5.1, we define the three experiments:

- **Rate vs. SNR:** The transmit power is fixed at $P = 1$ and the noise power σ^2 is varied such that the SNR (P/σ^2) sweeps from $-10\,\text{dB}$ to $20\,\text{dB}$. All other parameters are fixed (e.g., $M_t = 128$, $B = 128\,\text{MHz}$).
- **Rate vs. M_t:** The number of transmit antennas M_t is varied as $[32, 64, 128, 256]$. All other parameters are fixed (e.g., SNR $= 20\,\text{dB}$, $B = 128\,\text{MHz}$).
- **Rate vs. Bandwidth:** The system bandwidth B is varied as $[64, 128, 256, 512]$ MHz, which correspondingly changes the sampling time T_s. All other parameters are fixed (e.g., SNR $= 20\,\text{dB}$, $M_t = 128$).

5.2 Result 1: Achievable Rate vs. SNR

The first experiment evaluates the performance of the three models as the Signal-to-Noise Ratio (SNR) increases from $-10\,\text{dB}$ to $20\,\text{dB}$. The number of antennas ($M_t = 128$), number of RF chains ($M_{\text{RF}} = 8$), and bandwidth ($B = 128\,\text{MHz}$) are held at their default values as specified in Table 5.1.

The simulation results are presented in Figure 5.1. The plot shows four curves: the three hybrid beamformers (designed using the 'NB-DAM', 'SA-DAM', and 'WB-DAM' models, respectively) and the ideal, fully-digital benchmark ('WB-DAM (Digital)').

As expected, the `WB-DAM (Digital)` beamformer (black, dashed line) provides the upper-bound performance. It represents the theoretical maximum SINR achievable with the "ground truth" channel, unconstrained by a hybrid architecture, and thus serves as our ideal benchmark.

The key observation is that the `WB-DAM (Hybrid)` (blue, diamond) and `SA-DAM (Hybrid)` (red, square) curves track this ideal digital benchmark almost perfectly across the entire SNR range. The performance of the beamformer designed with the `SA-DAM` approximation is visually indistinguishable from the one designed with the "perfect" `WB-DAM` model. This yields two important insights:

- The OMP algorithm (detailed in Section 4.4) is highly effective at finding a hybrid approximation for the ideal beamformer. The minimal gap between the hybrid and digital

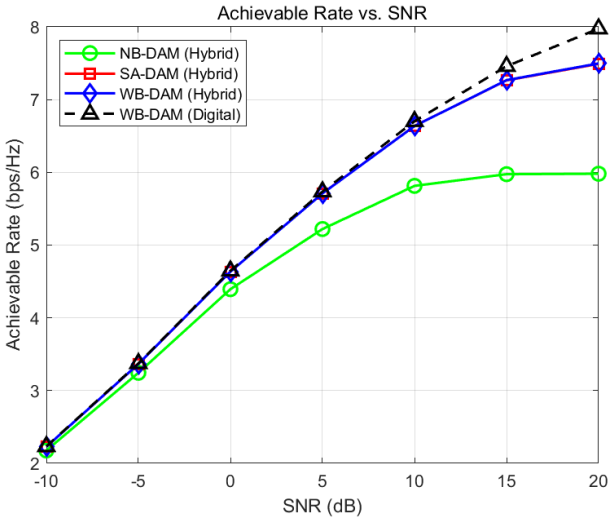

Figure 5.1: Achievable Rate vs. SNR for Hybrid and Digital Beamformers. All models are evaluated on the 'WB-DAM' ground truth channel.

`WB-DAM` curves shows that the $M_{\text{RF}} = 8$ RF chains are sufficient to capture the channel's spatial degrees of freedom.

- The `SA-DAM` model, which approximates the channel by sub-array (with $K = 8$), is a sufficiently-accurate model for this system configuration. The beamformer it produces has virtually identical performance to the one designed with the full wideband model.

In contrast, the `NB-DAM (Hybrid)` model (green, circle) exhibits a significant performance degradation, particularly at high SNR.

At low SNR (from -10 dB to 0 dB), the `NB-DAM` model performs reasonably well, as the system performance is primarily limited by the additive noise (σ^2). In this **noise-limited regime**, the modeling inaccuracies of `NB-DAM` are masked by the high noise floor.

However, as the SNR increases beyond 10 dB, the performance of the `NB-DAM` model saturates, hitting a "performance ceiling" at approximately 6.0 bps/Hz. This occurs because the system is no longer noise-limited; it has become **interference-limited**.

The `NB-DAM` model, by ignoring the spatial wideband effect, calculates an incorrect ideal beamformer $\mathbf{F}_{\text{opt}}^{\text{NB}}$. The resulting hybrid beamformer $(\mathbf{F}_{\text{RF}}^{\text{NB}}, \mathbf{F}_{\text{BB}}^{\text{NB}})$ is therefore not designed to null the true ISI of the wideband channel. At high SNR, this un-cancelled residual ISI becomes the dominant factor limiting the SINR, preventing any further increase in achievable rate. This

result clearly demonstrates that failing to account for the spatial wideband effect leads to a flawed beamformer design that performs poorly in high-SNR scenarios.

5.3 Result 2: Achievable Rate vs. Number of Antennas

The second experiment investigates the impact of the array aperture size on performance. We vary the number of transmit antennas M_t from 32 to 256, while keeping the SNR fixed at its default of 20 dB and the bandwidth at 128 MHz. Critically, the number of RF chains is held constant at $M_{\text{RF}} = 8$ for all hybrid models. The results are shown in Figure 5.2.

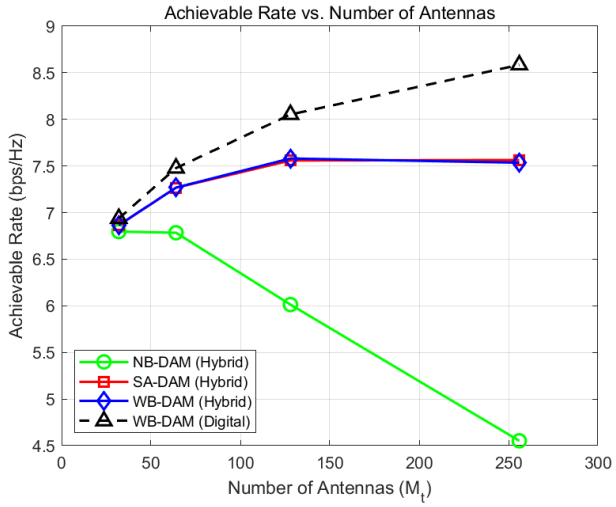

Figure 5.2: Achievable Rate vs. Number of Antennas (M_t). The SNR is fixed at 20 dB and $M_{\text{RF}} = 8$.

This experiment reveals the most significant finding of our study.

First, as the number of antennas M_t increases, the performance of the `NB-DAM (Hybrid)` model (green, circle) **collapses.** While it performs reasonably well for a small array ($M_t = 32$), its achievable rate drops sharply as the array size grows, falling to its lowest point at $M_t = 256$.

This behavior provides clear evidence of the spatial wideband effect. The `NB-DAM` model, which uses a single delay τ_l for all antennas, fails to recognize that the physical propagation delay is different for each antenna, as shown in (3.1). As the array size M_t increases, the physical distance between the first and last antenna grows, and the time difference $\tau_{l,M_t} - \tau_{l,1}$ becomes larger.

The NB-DAM model's assumption becomes increasingly incorrect, leading to a severely flawed beamformer design. This flawed beamformer fails to align the taps in time at the receiver, creating massive residual ISI that overwhelms the system and destroys the achievable rate. This confirms that for large-scale antenna arrays, the NB-DAM model is not just suboptimal; it is fundamentally incorrect and leads to system failure.

In contrast, the SA-DAM (red, square) and WB-DAM (blue, diamond) models are robust to the increase in antenna elements. Both models successfully account for the per-antenna delay variations—the WB-DAM perfectly and the SA-DAM as a close approximation. As a result, they both design effective beamformers that correctly align the channel taps, and their performance remains high and stable.

A final observation is the performance gap between the hybrid models and the ideal WB-DAM (Digital) benchmark (black, dashed line). The digital beamformer's rate scales with M_t because it can exploit the full **array gain** of the larger aperture. The hybrid models, however, flatten out around 7.6 bps/Hz. This is because their performance is ultimately constrained by the fixed number of RF chains ($M_{\text{RF}} = 8$). While the larger array provides a better analog beam selection, the system cannot leverage the full array gain without more digital RF chains. Nonetheless, the SA-DAM and WB-DAM hybrid designs successfully avoid the performance collapse seen in the narrowband model, proving their necessity for large arrays.

5.4 Result 3: Achievable Rate vs. Bandwidth

In the final experiment, we analyze the impact of system bandwidth on model performance. We vary the bandwidth B from 64 MHz to 512 MHz , which in turn changes the sampling time $T_s = 1/B$. The SNR is fixed at 20 dB and the number of antennas is fixed at $M_t = 128$.

The results, shown in Figure 5.3, are just as dramatic as those in the previous section. We observe a catastrophic performance collapse for the **NB-DAM (Hybrid)** model (green, circle) as the bandwidth increases. In contrast, the SA-DAM and WB-DAM models remain highly effective and stable.

This failure is a direct consequence of the relationship between bandwidth and time resolution. The spatial wideband effect is fundamentally a 'time-delay' phenomenon, where a signal

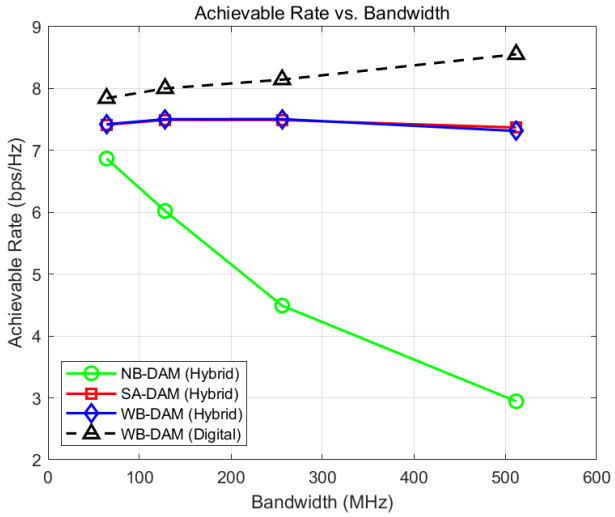

Figure 5.3: Achievable Rate vs. System Bandwidth (B). The SNR is fixed at 20 dB and $M_t = 128$.

arrives at different antennas at slightly different times ($\tau_{l,m}$). The system's "view" of this effect is determined by the sampling period T_s.

- **At Low Bandwidth ($B = 64$ MHz):** The sampling period T_s is relatively long. The small per-antenna time delays are "sub-tap" (i.e., $\tau_{l,M_t} - \tau_{l,1} < T_s$). The `NB-DAM` model's assumption that all delays are identical is a "good enough" approximation, so it performs reasonably well (though still worse than the other models).

- **At High Bandwidth ($B = 512$ MHz):** The sampling period T_s is now very short. The physical time delay across the array, which the `NB-DAM` model 'ignores', now spans 'multiple taps'. The model's assumption is no longer just inaccurate; it is fundamentally wrong.

Because the `NB-DAM` model is "blind" to this tap-spreading, it designs a beamformer $\mathbf{F}_{\text{opt}}^{\text{NB}}$ that fails to align the taps of the true wideband channel. This creates a massive amount of un-cancelled ISI, which, as seen in the 20 dB SNR (interference-limited) regime, dominates the system and causes the achievable rate to plummet.

Once again, the `SA-DAM (Hybrid)` (red, square) and `WB-DAM (Hybrid)` (blue, diamond) models are robust to this change. Because they correctly model the per-antenna (or per-sub-array) delays, their beamformer designs remain valid and effective even as T_s shrinks. Their performance is stable, with the `SA-DAM` model again proving to be an excellent approximation of the

full WB-DAM model.

Finally, the ideal WB-DAM (Digital) benchmark (black, dashed line) shows a slight increase in rate as bandwidth grows. This is expected, as a wider bandwidth provides higher time resolution, which allows the system to resolve more multi-path components, increasing the channel's frequency diversity. The fully-digital system can exploit this, while the hybrid models are limited by their $M_{\mathrm{RF}} = 8$ RF chains.

5.5 Result 4: Computational Complexity and Runtime Analysis

While the previous results demonstrate the superior spectral efficiency of the SA-DAM and WB-DAM models, the computational cost of beamforming optimization is also a critical metric for system realizability. A common concern is that physically accurate wideband models might incur a prohibitive computational cost compared to the simpler narrowband approximation.

To investigate this, we conducted a "stress test" simulation with increased channel density. We increased the number of multi-paths to $L = 20$ (compared to the default $L = 4$) and the number of RF chains to $M_{\mathrm{RF}} = 40$, decreased the tap selection threshold to $C = 0.001$. This setup increases the diversity of the channel, allowing us to more effectively evaluate runtime differences.

The average optimization runtime per channel realization for each model is presented in Table 5.2.

Table 5.2: Average Optimization Runtime ($L = 20$, $M_{\mathrm{RF}} = 40$)

Model	**Avg. Hybrid SINR (dB)**	**Avg. Ideal SINR (dB)**	**Avg. Runtime (s)**
NB-DAM	24.56	24.57	2.15
SA-DAM	33.22	35.31	2.02
WB-DAM	33.58	35.39	2.01

The results indicate that there is no significant runtime penalty for using the more accurate SA-DAM or WB-DAM models. In fact, the runtimes are remarkably similar, with the WB-DAM model actually performing slightly faster on average in this specific case.

This similarity can be explained by analyzing the computational bottleneck of the beam-

forming design. As detailed in Chapter 4, the core of the optimization involves calculating the MMSE beamformer $\bar{\mathbf{f}}^{\mathrm{MMSE}}$, which requires the inversion of the interference-plus-noise covariance matrix $\mathbf{C}$ defined in (**??**).

The dimension of matrix $\mathbf{C}$ is $(M_t L' \times M_t L')$, where M_t is the number of antennas and L' is the number of *selected* effective taps (clusters) to be aligned. The computational complexity of identifying these taps (clustering) is negligible compared to the $O((M_t L')^3)$ complexity of inverting $\mathbf{C}$. Therefore, the runtime is primarily dominated by the value of L'.

In our simulations, despite the differences in physical accuracy, all three models tended to identify and select a similar number of dominant taps (L') from the channel. Because L' remains similar across the three models, the size of the matrix $\mathbf{C}$ remains similar, leading to nearly equivalent computational loads.

This is a significant finding for practical implementation. It demonstrates that the performance gains of `SA-DAM` and `WB-DAM` (an approximate 9 dB SINR gain in this scenario) can be achieved without incurring additional computational delay, making them highly attractive for real-time wideband systems.

Chapter 6 Conclusion

This thesis has conducted a comprehensive investigation into the practical design of hybrid analog/digital beamformers for Delay Alignment Modulation (DAM) systems, focusing on the critical, but often-overlooked, spatial wideband effect. As mmWave and THz systems move towards larger antenna arrays (M_t) and wider bandwidths (B), this effect, also known as "beam squint," introduces per-antenna time delays that can severely degrade system performance if not properly modeled.

Our work sought to answer a fundamental question: how much does channel model accuracy matter when designing a practical, hybrid beamformer?

To answer this, we implemented and compared three distinct channel models within a full Monte Carlo simulation environment:

1. **'NB-DAM':** The traditional narrowband model, which ignores the spatial wideband effect entirely.
2. **'WB-DAM':** The "ground truth" wideband model, which accurately computes a unique delay for every single antenna element.
3. **'SA-DAM':** A proposed intermediate model that approximates the channel by partitioning the array into sub-blocks, each sharing a single representative delay.

Our methodology was to design a practical hybrid beamformer using each of these three models (via OMP) and then, critically, evaluate all three on the "ground truth" `WB-DAM` channel to measure their real-world performance.

6.1 Summary of Findings and Contributions

The simulation results from Chapter 5 led to several clear and significant conclusions. The primary contributions of this thesis are:

- **This work provides a definitive quantification of the failure of narrowband models for wideband systems.** Our results in Section 5.3 and Section 5.4 are clear. The

`NB-DAM` model, which is the "default" assumption in much of the literature, is completely non-viable for large-scale DAM systems. Its performance does not merely degrade; it collapses catastrophically as M_t or B increases. We demonstrated that this is because the flawed model designs a beamformer that fails to cancel the true ISI of the wideband channel, leading to a performance ceiling in an interference-limited regime.

- **This work validates the `SA-DAM` model as a highly-effective and computationally-efficient alternative.** Across all experiments (SNR, M_t, and B), the performance of the hybrid beamformer designed with the `SA-DAM` approximation was nearly identical to the one designed with the "perfect" `WB-DAM` model. This is a crucial finding, as it provides a practical path forward for system designers. It proves that one does not need to bear the full accuracy of the per-antenna `WB-DAM` model; a simpler sub-array approximation is sufficient to capture the essential physics and achieve near-optimal performance.

- **This work demonstrates the robustness of hybrid beamforming approximation (OMP) for DAM systems.** A secondary finding was that for a system with $L = 4$ paths, $M_{\text{RF}} = 8$ RF chains were sufficient to design a hybrid beamformer that closely tracked the performance of the ideal, fully-digital benchmark, especially in the low-to-mid SNR range.

In summary, this thesis has shown that while the spatial wideband effect is a system-breaking challenge, it is one that can be successfully overcome. The traditional narrowband assumption is obsolete for these systems, but a `SA-DAM` approximation provides a robust and practical solution.

6.2 Limitations and Future Work

This research opens several avenues for future investigation:

- **Optimal Sub-Array Partitioning:** Our `SA-DAM` model used a fixed number of sub-arrays ($K = 8$). A future study could investigate the optimal K, analyzing the trade-off between model complexity (increasing K) and achievable rate.

- **Impact of Imperfect CSI:** Our simulation assumed perfect knowledge of the channel's physical parameters (AoDs) to build the OMP dictionary. A crucial next step would be to

evaluate these models in a scenario with realistic channel estimation errors.

- **Multi-User (MU-MIMO) Scenarios:** This work focused on a single-user (MISO) link. Expanding this analysis to a multi-user scenario would be highly valuable, as the beamformers would need to manage both ISI and multi-user interference, placing even greater stress on the channel model's accuracy.

Bibliography

[1] J. Zhang et al., "Delay alignment modulation with hybrid analog/digital beamforming for millimeter wave and terahertz communications," *IEEE Transactions on Wireless Communications*, vol. 24, no. 9, pp. 7360–7376, 2025. DOI: 10.1109/TWC.2025.3560150

[2] I.-S. Kim and J. Choi, "Spatial wideband channel estimation for mmwave massive mimo systems with hybrid architectures and low-resolution adcs," *IEEE Transactions on Wireless Communications*, vol. 20, no. 6, pp. 4016–4029, 2021. DOI: 10.1109/TWC.2021.3054998

[3] O. E. Ayach, S. Rajagopal, S. Abu-Surra, Z. Pi, and R. W. Heath, "Spatially sparse precoding in millimeter wave mimo systems," *IEEE Transactions on Wireless Communications*, vol. 13, no. 3, pp. 1499–1513, 2014. DOI: 10.1109/TWC.2014.011714.130846

초 록

지연 정렬 변조(Delay Alignment Modulation, DAM)는 채널의 다중 경로 희소성(sparsity)을 활용하여 밀리미터파(mmWave) 및 테라헤르츠(THz) 통신에서 심볼 간 간섭(Inter-Symbol Interference, ISI)을 완화하는 유망한 기술이다. 기존 연구들은 DAM의 이론적 이점을 입증했으나, 실제 시스템 구현을 위해서는 하이브리드 아날로그/디지털 빔포밍의 하드웨어적 제약과 빔 스퀸트(beam squint)로 알려진 공간 광대역 효과(spatial wideband effect)라는 두 가지 주요 과제를 해결해야 한다. 특히 대규모 안테나 배열과 광대역을 사용하는 시스템에서는 공간 광대역 효과로 인해 안테나 소자마다 서로 다른 전파 지연이 발생하게 되며, 이는 기존의 협대역(narrowband) 가정이 더 이상 유효하지 않음을 의미한다.

본 논문에서는 채널 모델의 정확도가 DAM 시스템을 위한 실용적 하이브리드 빔포머 설계에 미치는 영향을 분석한다. 이를 위해 안테나별 지연을 무시하는 기존의 협대역 모델(NB-DAM), 이를 완벽하게 반영하는 광대역 모델(WB-DAM), 그리고 이를 근사화한 서브 어레이 모델(SA-DAM)의 세 가지 모델을 정립하고 비교하였다. 각 모델을 기반으로 직교 매칭 (Orthogonal Matching Pursuit, OMP) 알고리즘을 통해 하이브리드 빔포머를 설계하고, 전송률(achievable rate) 성능을 평가하였다. 시뮬레이션 결과, 기존 협대역 모델은 안테나 수나 대역폭이 증가함에 따라 실제 광대역 ISI를 제거하지 못하여 성능이 급격히 저하됨을 확인하였다. 반면, 제안된 서브 어레이 근사 모델(SA-DAM)은 전체 광대역 모델(WB-DAM)과 대등한 성능을 보이면서도 연산 효율성이 뛰어나, 실제 대규모 밀리미터파 시스템을 위한 효과적인 솔루션임을 입증하였다.

주요어:지연 정렬 변조, 하이브리드 빔포밍, 공간 광대역 효과, 심볼 간 간섭, 밀리미터파 통신, 서브 어레이 구조